# Toward CMOS-Compatible Triboelectric Generator to Operate MEMS

Mohammad Alzgool

Department of Mechanical Engineering
Binghamton University
Binghamton, USA
Email: malzgoo1@binghamton.edu

Mohammad Mousavi

Department of Mechanical Engineering
Binghamton University
Binghamton, USA
Email: smousav1@binghamton.edu

Benyamin Davaji

Electrical and Computer Engineering

Northeastern University

Boston, USA

b.davaji@northeastern.edu

Shahrzad Towfighian

Department of Mechanical Engineering

Binghamton University

Binghamton, USA Email: stowfigh@binghamton.edu

Abstract-In this paper, a shock detector is introduced using a micro-scale triboelectric generator and an electrostatic MEMS switch. The fabrication of a micro-scale tribo-electricnano generator is carried out using MEMS technology for the first time. The fabrication technique enabled reducing the size by 85% compared to a prior work. The generator has aluminumpolyimide on the bottom layer, a gap, and a top layer of Al and amorphous silicon (a-Si). The generator produces 0.4 Vpulses as a response to impulse excitation, the produced voltage is used to trigger switch closure by adding it to a DC voltage that is enough to bend the beam down but not enough to close it. The combination of MEMS-triboelectric generator and MEMS electrostatic actuators is ideal because both are fabricated with CMOS technology and can be integrated on the same chip. The proposed system enables creating event-powered micro-switches. Index Terms—TENG, Tribo-electric-nano-generator, MEMS, shock sensing, actuators, self-powered, polyimide.

## I. Introduction

Nowadays, the focus of research on energy harvesting is rapidly increasing because of the increasing demand resulted from the increased number of sensors and actuators worldwide. In the of Internet of Things (IoT), billions of wireless sensors and actuators are interconnected to create a network. The aim of energy harvesting research is to find the best mechanism to maximize the energy and minimize the impact on the environment. [1]

While many energy harvesting mechanisms have been invented to harvest mechanical energy, the most studied are electromagnetic harvesters [2], piezo-electric energy harvesters (PEHs) [3]–[5], the triboelectric energy harvesters (TEHs) [6]–[10], and hybrid harvesters [11]–[14]. The energy harvesters were introduced into various applications including traffic safety [3], motion energy [2], [6], [13], vibration measurement [4], and water energy harvesting [5], [14].

The authors would like to acknowledge the financial support of the National Science Foundation (NSF) through Grant #1919608. This work was performed in part at the Cornell NanoScale Science and Technology Facility, a member of the National Nanotechnology Coordinated Infrastructure, which is supported by the National Science Foundation (Grant NNCI-2025233).

Compared to other types of generators, the triboelectric generators have great advantages because of the simple fabrication process, their low-cost, and their integrability into systems [9]. TENGs have many operating modes; single-electrode mode [11], [13], sliding mode [14], rotary mode [9], and contact-separation mode [6]–[8], [10]. All the working modes of the TENGs rely on the electrification of a triboelectric pair, this pair is made of two conductive electrodes and a dielectric material. There is a large selection of dielectric materials, the most commonly studied dielectric material are polyte-trafluoroethylene (PTFE) [6]–[8], [10], polydimethylsiloxane (PDMS) [13], and polyimide [12]. Other less studied dielectric materials include ionic hydrogel [15], [16], polymethyl methacrylate (PMMA) [17], Nylon [18], and paper [19].

When dielectric materials come in contact with a conductive material, they get oppositely charged. Then, when the contact is lost between the conductive and dielectric material, charge distribution create potential difference between two conductors.

The TENGs are included in many self-powered devices studies where they are used for sensing and actuation. For instance; Yao et. al used contact-separation TENG to harvest energy from walking to power a attached tracking device [10], Yeh et. al used TENG to power waste collecting device in the ocean [9], and we used a contact-separation bi-stable mechanism to create autonomous shock sensor in macro-scale [20].

In 2019, Hamid et al. [21], [22] used UV-LIGA technology to fabricate a triboelectric generator that had a smaller size compared to the previous designs. The top electrode of their design was rectangular-shaped and its dimensions were 3  $mm \times 5 \ mm \times 10 \ \mu m$  with a triboelectric pair of Polydimethylsiloxane (PDMS) and aluminum (Al). In this work, we will demonstrate the fabrication of a contact-separation mode triboelectric generator in micro-scale fabricated with Micro-electromecahnical-systems (MEMS) technology, which reduced the area by 85% (square top-electrode is  $1.5mm \times 1.5mm \times 1\mu m$ ). The triboelectric pair of polyimide (PI) and Al is compatible

with the MEMS technology and enabled miniaturization of the device. Furthermore, we will show how this mico-scale generator is utilized as a shock detector by actuating a MEMS switch under the effect of a mechanical shock.

### II. FABRICATION

Contact-separation mode triboelectric generators are made of a triboelectric material on a conductive plate and another conductive layer separated by a gap. In this work, the contactseparation MEMS-triboelectric generator was made of a bottom electrode of Al/PI and a top electrode of Al/a-Si, Al serves as the two conductive electrodes, PI forms triboelectric pair with the bottom Al electrode, and a-Si serves as a mass on top of the upper Al electrode to increase kinetic energy harvesting. The fabrication process is shown in Fig.1, we start with a 4-inch Si wafer with an insulating film of aluminum nitride (AlN) that separates the device from the silicon wafer, a DC sputtering (s) film of chromium and aluminum (Cr/Al) was deposited on the AlN layer, (a). This layer was patterned by inductive conductive plasma machine (ICP) to form the bottom electrode, (b). Then, 5  $\mu m$  thick PI was coated on top of the Cr/Al layer by spin-coating PI precursor and oven-baking it in PI-oven, (c). Then, the PI was patterned using reactive ion etching machine (RIE), (d). After the PI was patterned, 2  $\mu m$ silicon oxide was deposited on PI to form the gap with plasma enhanced chemical vapor deposition (PECVD), (e). The oxide layer was patterned to form anchors ,(f), and pins, (g), with RIE. The pins are created by etching 1  $\mu m$  holes into the oxide layer on top. To form top electrode conductive layer,  $120 \ nm$ s-film of Cr/Al was deposited on top, (h). Then, the Cr/Al layer was etched to form the top electrode with ICP, (i). PECVD film of a-Si was deposited on top, (j). Recipe used for (j) was chosen to get tensile film stress to avoid breaking when the oxide is removed. a-Si was etched to open contact-pads using RIE, (k). Then, both Cr/Al and a-Si layers were etched again using RIE and ICP to create release holes, (1). These release holes increase the area exposed to vapor hydro-fluoride acid used for oxide removal, (m). To test the generator, a MEMS

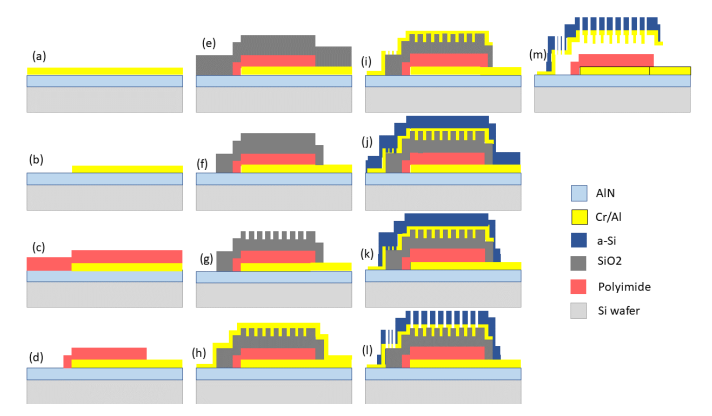


Fig. 1. Fabrication process of the MEMS-triboelectric generator.

electrostatic actuator was used [20], this actuator was made by PolyMUMPs from MEMSCAP. The actuator was used as a

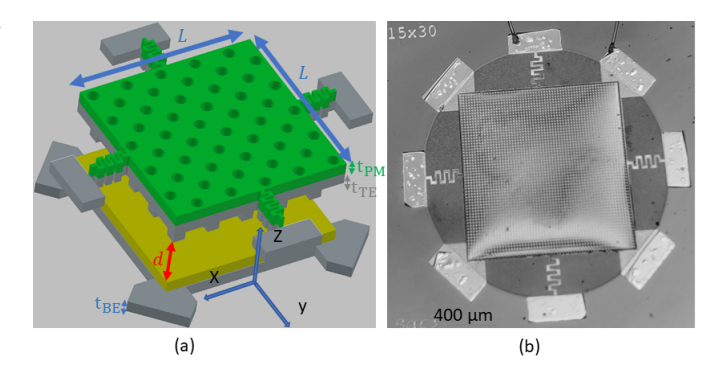


Fig. 2. (a) 3D schematic of the MEMS-triboelectric generator, (b) image of the fabricated MEMS-triboelectric generator.

parallel-plate MEMS switch with moving electrode that is 500  $\mu m \times 20 \mu m \times 2 \mu m$ , the actuator also has two side electrodes that cause the beam to move up when voltage is applied to them, this enables beam release if it got pulled-in.

A 3D schematic and an optical image of the fabricated device are shown in Fig. 2. The dimensions of the MEMS-triboelectric generator design are summarized in Table. I.

Description	Symbol	Design Value	Material
Top electrode length	L	$1.5 \ mm$	
Bottom conductive thickness	$t_{BE}$	$200 \ nm$	Cr/Al
Tribo-layer thickness	$t_T$	$5 \mu m$	PI
Separation gap	d	$2 \mu m$	$SiO_2$
Top conductive thickness	$t_{TE}$	$100 \ nm$	Cr/Al
Proof mass thickness	$t_{PM}$	$1 \mu m$	a-Si
Switch Length	l	$500 \ \mu m$	
Switch width	w	$20 \ \mu m$	
Switch thickness	b	$2  \mu m$	
	TABLE I		

DESIGN DIMENSIONS OF THE MEMS-TRIBOELECTRIC GENERATOR.

The advantages of our design are; the gap fabricated in using silicon oxide which is easy to etch out, the top electrode was only 1  $\mu m$  in thickness, and the fabrication was conducted in nano-fabrication facility which makes the generator compatible with MEMS technology.

## III. TESTING SETUP

For testing the fabricated MEMS-triboelectric generator, the generator is fixed on top of the stage of an electro-dynamic shaker (BK 4810) driven by a power amplifier (Krohn-Hite 7600). A USB data acquisition system (DAQ) was used to apply inputs to the amplifier and a summer circuit. The summer circuit inputs are connected to the DAQ and the MEMS-triboelectric generator and the output was fed to the MEMS-switch. A laser-doppler vibrometer (MSA500) is used to measure the displacement of the switch where the measurement signal is received by the DAQ. The test setup schematic is shown in Fig. 3.

# IV. RESULTS AND ANALYSIS

The fabricated generator was tested with impulse excitation from the shaker, the open-circuit measurement for an impulse of 0.5V is shown in Fig. 4. We notice that the output voltage

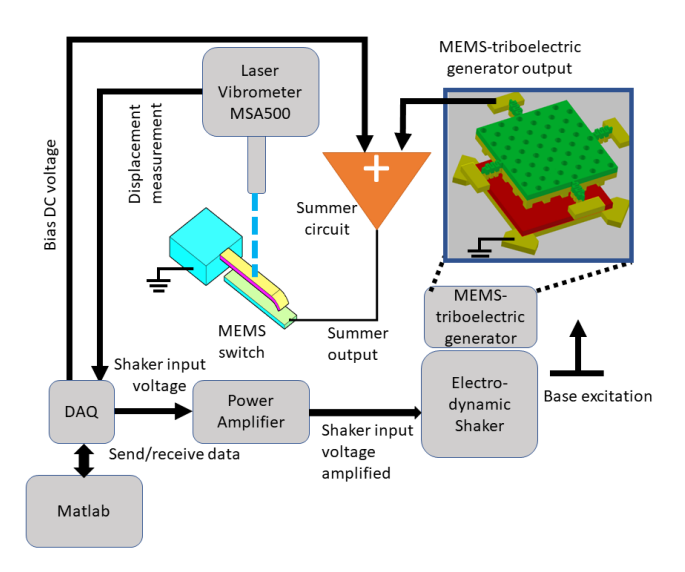


Fig. 3. Experimental setup schematic.

from the MEMS-triboelectric generator has a peak around 0.4 V and decays 0.4 msec. As reported in [23], the pull-in voltage of the MEMS switch we used for this experiment was 2.25 V. A summer circuit is used to add a bias voltage to the generated voltage to keep the MEMS switch close to its pull-in threshold. In theory, an additional 1.85 V is needed to cause the pullin. When applying the bias voltage, the MEMS switch bends down electrostatically but does not collapse unless enough bias voltage (pull-in voltage) is applied. However, when the experiment was conducted with bias voltage less than 2.24 V, the switch does not close because the fast decay of the generated voltage causes the beam response to revert back. Because of the dynamic behavior of the generated voltage, a static bias DC voltage of was added to the pulse produced from the MEMS-triboelectric generator. DC voltage of 2.24 V was required to close the switch as a response to the impulse excitation. Fig. 5 shows the impulse excitation result when the switch is pulled-in and when it reverted back to initial displacement.

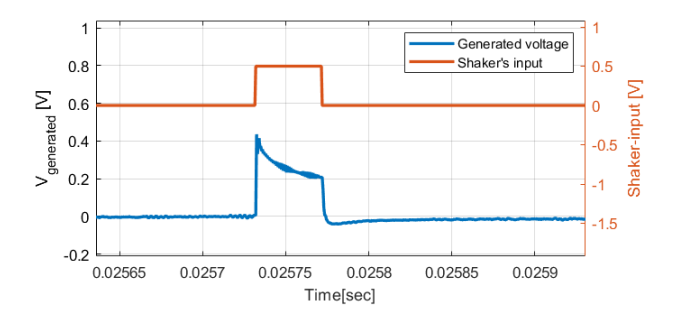


Fig. 4. Time history of impulse excitation and MEMS-triboelectric generator generated voltage.

The DC voltage to the MEMS switch provides tunability. By setting the DC voltage to proper value, the amplitude that causes the switch to close can be adjusted. We notice

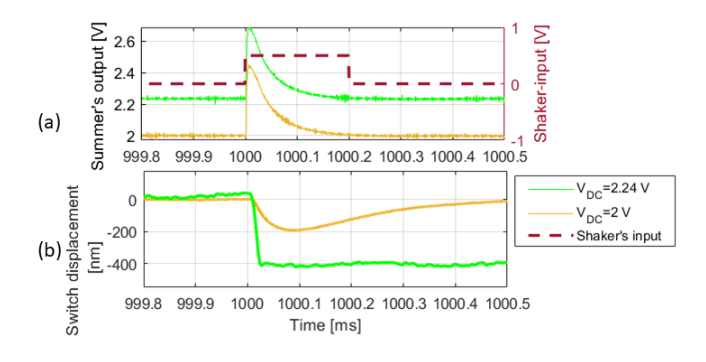


Fig. 5. (a) Time history of impulse applied to the shaker, (b) summer-circuit output, and (c) switch displacement. Part (c) shows that the DC voltage makes switch tunable to the shock it receives.

that motion resulted from the same generated voltage increase when  $V_{DC}$  is increased, this happens because the beam becomes more prone to shocks. As the plates get closer, the nonlinear electrostatic force increases. When 2 Vs is applied, the impulse causes the beam to move down for 200 nm, increasing the voltage to 2.24 V, the same impulse induces 400 nm motion and causes the beam to get pulled-in. In Fig. 5, switch displacement is set to reference value (0) to compare beam response at different  $V_{DC}$ s and to minimize measurement errors of displacement drifting from phase-shift based doppler measurement. Even though the system requires bias voltage to cause switch to close, the electrostatic actuators do not require current and, thus, require low-power to operate.

# V. CONCLUSION

We presented a shock detection system that is made by a contact-separation triboelectric generator fabricated in microscale and an electrostatic MEMS actuator. The fabrication process of the triboelectric generator is conducted in a nanofabrication facility using CMOS compatible process. The mechanical energy of a shock iss harvested by the MEMS-triboelectric generator and it is used to close the parallel-plate electrostatic actuator. The reported generator has a 1.5  $mm \times 1.5 \ mm \times 1 \ \mu m$  top electrode, this generator is the smallest reported generator and it has a triboelectric pair of aluminum and polyimide which makes it compatible with MEMS fabrication process and integration of several components on the same chip. The generator can be employed to drive event-powered sensors that has low-power requirement.

### REFERENCES

- Slabov, V., Kopyl, S., Soares dos Santos, M. P., and Kholkin, A. L., 2020.
   "Natural and eco-friendly materials for triboelectric energy harvesting".
   Nano-Micro Letters, 12(1), pp. 1–18.
- [2] Fan, K., Cai, M., Liu, H., and Zhang, Y., 2019. "Capturing energy from ultra-low frequency vibrations and human motion through a monostable electromagnetic energy harvester". *Energy*, 169, pp. 356–368.
- [3] Wang, C., Wang, S., Gao, Z., and Wang, X., 2019. "Applicability evaluation of embedded piezoelectric energy harvester applied in pavement structures". Applied Energy, 251, p. 113383.
- [4] Zhou, J., Zhao, X., Wang, K., Chang, Y., Xu, D., and Wen, G., 2021. "Bio-inspired bistable piezoelectric vibration energy harvester: Design and experimental investigation". *Energy*, 228, p. 120595.
- [5] Shan, X., Li, H., Yang, Y., Feng, J., Wang, Y., and Xie, T., 2019. "Enhancing the performance of an underwater piezoelectric energy harvester based on flow-induced vibration". *Energy*, 172, pp. 134–140.
- [6] Zhang, S., Xu, J., Yu, J., Song, L., He, J., Ma, N., Hou, X., and Chou, X., 2021. "An all-rubber-based woven nanogenerator with improved triboelectric effect for highly efficient energy harvesting". *Materials Letters*, 287, p. 129271.
- [7] Zhao, C., Yang, Y., Upadrashta, D., and Zhao, L., 2021. "Design, modeling and experimental validation of a low-frequency cantilever triboelectric energy harvester". *Energy*, 214, p. 118885.
- [8] Zhao, H., and Ouyang, H., 2021. "A capsule-structured triboelectric energy harvester with stick-slip vibration and vibro-impact". *Energy*, 235, p. 121393.
- [9] Yeh, M.-H., Guo, H., Lin, L., Wen, Z., Li, Z., Hu, C., and Wang, Z. L., 2016. "Rolling friction enhanced free-standing triboelectric nanogenerators and their applications in self-powered electrochemical recovery systems". Advanced Functional Materials, 26(7), pp. 1054– 1062.
- [10] Yao, M., Xie, G., Gong, Q., and Su, Y., 2020. "Walking energy harvesting and self-powered tracking system based on triboelectric nanogenerators". *Beilstein Journal of Nanotechnology*, 11(1), pp. 1590– 1595
- [11] Jiang, D., Su, Y., Wang, K., Wang, Y., Xu, M., Dong, M., and Chen, G., 2020. "A triboelectric and pyroelectric hybrid energy harvester for recovering energy from low-grade waste fluids". *Nano Energy*, 70, p. 104459.
- [12] Sun, Y., Lu, Y., Li, X., Yu, Z., Zhang, S., Sun, H., and Cheng, Z., 2020. "Flexible hybrid piezo/triboelectric energy harvester with high power density workable at elevated temperatures". *Journal of Materials Chemistry A*, 8(24), pp. 12003–12012.
- [13] Ji, S. H., Lee, W., and Yun, J. S., 2020. "All-in-one piezo-triboelectric energy harvester module based on piezoceramic nanofibers for wearable devices". ACS Applied Materials & Interfaces, 12(16), pp. 18609– 18616.
- [14] Wu, Z., Guo, H., Ding, W., Wang, Y.-C., Zhang, L., and Wang, Z. L., 2019. "A hybridized triboelectric–electromagnetic water wave energy harvester based on a magnetic sphere". ACS nano, 13(2), pp. 2349– 2356.
- [15] Pu, X., Liu, M., Chen, X., Sun, J., Du, C., Zhang, Y., Zhai, J., Hu, W., and Wang, Z. L., 2017. "Ultrastretchable, transparent triboelectric nanogenerator as electronic skin for biomechanical energy harvesting and tactile sensing". Science advances, 3(5), p. e1700015.
- [16] Shuai, L., Guo, Z. H., Zhang, P., Wan, J., Pu, X., and Wang, Z. L., 2020. "Stretchable, self-healing, conductive hydrogel fibers for strain sensing and triboelectric energy-harvesting smart textiles". *Nano Energy*, 78, p. 105389.
- [17] Varghese, H., and Chandran, A., 2021. "A facile mechanical energy harvester based on spring assisted triboelectric nanogenerators". Sustainable Energy & Fuels, 5(20), pp. 5287–5294.
- [18] Choi, Y. S., and Kar-Narayan, S., 2020. "Nylon-11 nanowires for triboelectric energy harvesting". *EcoMat*, 2(4), p. e12063.
- [19] Wu, C., Kima, T. W., Sung, S., Park, J. H., and Li, F., 2018. "Ultrasoft and cuttable paper-based triboelectric nanogenerators for mechanical energy harvesting". *Nano Energy*, 44, pp. 279–287.
- [20] Mousavi, M., Alzgool, M., and Towfighian, S., 2021. "Autonomous shock sensing using bi-stable triboelectric generators and mems electrostatic levitation actuators". Smart Materials and Structures, 30(6), p. 065019.

- [21] Hamid, H. A., and Celik-Butler, Z., 2019. "Design and optimization of a mems triboelectric energy harvester for nano-sensor applications". In 2019 IEEE Sensors Applications Symposium (SAS), IEEE, pp. 1–6.
- [22] Hamid, H. A., and Çelik-Butler, Z., 2020. "A novel mems triboelectric energy harvester and sensor with a high vibrational operating frequency and wide bandwidth fabricated using uv-liga technique". Sensors and Actuators A: Physical, 313, p. 112175.
- [23] Mousavi, M., Alzgool, M., and Towfighian, S., 2021. "Electrostatic levitation: an elegant method to control mems switching operation". *Nonlinear Dynamics*, 104(4), pp. 3139–3155.